Future Foods 12 (2025) 100759

Contents lists available at ScienceDirect

Future Foods

journal homepage: www.elsevier.com/locate/fufo

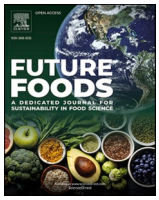

Integrating metabolomics and physicochemical analysis in black soldier fly bioconversion of *Schizochytrium* residue: A pathway to high-value ω-3 products

Yaru Zhang [a,1], Jing Liu [a,1], Yan Xiao [b], He Yang [a], Yanzhou Zhang [b], Chrysantus Mbi Tanga [c], Dawei Huang [a], Jinhua Xiao [a,*]

[a] College of Life Science, Nankai University, Tianjin 300071, China
[b] Institute of Zoology, Chinese Academy of Sciences, Beijing 100101, China
[c] International Centre of Insect Physiology and Ecology (icipe), Nairobi, Kenya

ARTICLE INFO

Keywords:
Black soldier fly larvae
Schizochytrium residue
ω-3 fatty acids
Physicochemical properties
Metabolomics

ABSTRACT

The global microalgae processing industry generates substantial residues rich in ω-3 fatty acids, presenting both a waste management challenge and an untapped resource for innovative food biotechnology. This study investigated the potential of bioconversion of *Schizochytrium* residue (SCR) by black soldier fly larvae (BSFL) to enrich ω-3 fatty acids and evaluated the industrial applicability of the resulting BSFL products. SCR supplementation enhanced larval growth performance (7.5 % increased weight, 19.9 % higher bioconversion rate) and protein quality, while enabling exclusive accumulation of EPA and DHA in BSFL. The total ω-3 content increased from 1.18 % to 17.37 %, achieving a nutritionally favorable n-6/n-3 ratio of 0.62 (the recommended ratio for human health <5). Metabolomics revealed that SCR upregulated TCA cycle intermediates and CoA biosynthesis, promoting FA synthesis, but NADPH limitations inhibited endogenous ω-3 elongation, suggesting direct assimilation of dietary PUFAs rather than de novo synthesis. Physicochemical analyses revealed improved thermal stability and β'-crystal formation in SCR-derived lipids. This work establishes a sustainable, technology-driven strategy for valorizing algal waste into nutritionally enhanced food ingredients, bridging the gap between circular bioeconomy principles and next-generation food production.

1. Introduction

The global microalgae processing industry generates substantial residues annually (Ali, 2022). Among these, *Schizochytrium* sp., a primary strain for industrial production of ω−3 fatty acids (ω−3 FAs) (Zhu et al., 2017), yields processing residues still abundant in underutilized bioactive compounds. Global demand for docosahexaenoic acid (DHA, C22:6n3) and eicosapentaenoic acid (EPA, C20:5n3) has exceeded 241, 000 t (Panse and Phalke, 2016), highlighting the urgency for sustainable management of *Schizochytrium* residues (SCR). Conventional disposal methods, such as composting and anaerobic digestion (Matsakas et al., 2017), exhibit critical limitations, including inefficient utilization of ω−3 FAs and environmental risks from leachate contamination. While some recently developed techniques, such as hydrothermal liquefaction, can extract bioactive compounds from microalgal residues, their high costs hinder widespread adoption (Narayanan, 2024).

Black soldier fly larvae (*Hermetia illucens*, BSFL) have emerged as a promising solution for organic waste valorization due to their high bioconversion efficiency (Tepper et al., 2024; Wu et al., 2024). BSFL convert organic waste into protein-rich (40–43 %) and lipid-rich (21–38 %) biomass (Heffernan, 2017; Spranghers et al., 2017). However, their native lipids are dominated by lauric acid (C12:0, 31–54 %) with minimal ω−3 FA content (0.5–3.2 %) (Barroso et al., 2017; Liland et al., 2017; Zhang et al., 2025a). Nevertheless, substrate optimization offers potential for nutritional enhancement (Ewald et al., 2020; Huang et al., 2025). Compared to traditional methods, BSFL-based processing reduces carbon footprints while improving resource efficiency (Salomone et al., 2017; Tzachor et al., 2021).

Numerous studies confirm BSFL's efficacy in converting food waste and agricultural byproducts (Meneguz et al., 2018). Feeding ω−3

* Corresponding author.
E-mail address: xiaojh@nankai.edu.cn (J. Xiao).
[1] Yaru Zhang and Jing Liu contributed equally.

https://doi.org/10.1016/j.fufo.2025.100759
Received 22 May 2025; Received in revised form 9 September 2025; Accepted 12 September 2025
Available online 13 September 2025

enriched substrates significantly elevates ω−3 FA content in BSFL (St-Hilaire et al., 2007). For instance, El-Dakar et al. (2021) demonstrated BSFL's ability to accumulate ω−3 FAs (25–31 % linolenic acid) when fed silkworm pupae. A dietary n-6/n-3 ratio below 5 is optimal for human health; while crickets and mealworms require 2 % flaxseed oil supplementation to achieve this ratio, BSFL achieve it with only 1 % (Oonincx et al., 2020). Recent studies on SCR valorization via BSFL reveal that 50 % SCR inclusion elevates ω−3 FA content to 11.8 % (El-Dakar et al., 2020). Furthermore, 10 % SCR in brewer's spent grain enhances DHA content to 6.7 % while shortening larval development time from 16 to 13 days (Ceccotti et al., 2022). However, existing research predominantly focuses on macronutrient quantification, neglecting small-molecule metabolites. Systematic evaluation of the physicochemical properties of black soldier fly larval oil (BSFLO) and larval slurry remains insufficient, and the metabolic pathways underlying bioactive compound enrichment are poorly understood.

This study aims to quantify BSFL's ω−3 FA enrichment efficiency from SCR and evaluate its industrial applicability through multi-scale analyses. A mass balance model (Bajra et al., 2023) was employed to assess larval growth performance (survival rate, bioconversion rate, protein conversion ratio) and dry mass reduction of substrate. Fourier transform infrared (FT-IR), differential scanning calorimetry (DSC), thermogravimetric analysis (TGA), and X-ray diffraction (XRD) were integrated to characterize BSFLO physicochemical properties, while ABTS/·OH radical scavenging assays and SOD/MDA activity measurements elucidated the antioxidant capacity of larval slurry. Moreover, metabolomics has been extensively employed in studies pertaining to resource optimization (Hussain et al., 2023; Noman and Azhar, 2023; Shah et al., 2024), HPLC-QE untargeted metabolomics identified key bioactive compounds and metabolic pathways.

The novelty of this work lies in: (1) pioneering the integration of macronutrient and metabolomic data to unravel SCR's impact on BSFL; (2) multidimensional characterization of the physicochemical properties of BSFLO and the antioxidant functionality of larval slurry; (3) screening critical bioactive compounds and metabolic pathways during bioconversion. These findings provide a theoretical foundation for SCR valorization and the development of tailored ω−3 enriched BSFL products, advancing circular economy and carbon neutrality goals.

2. Materials and methods

2.1. Materials source and preparation

The BSFL used in this study were sourced from a laboratory-reared population (Wuhan strain). Wheat bran and corn residue were provided by Huamo Biotechnology Co., Ltd. (Weifang, China), while SCR was purchased from Xi'an Xiaocao Plant Technology Co., Ltd. (Xi'an, China). The basal substrate for the control group (CG) was prepared by mixing wheat bran and corn residue at a 2:1 dry weight ratio. For the experimental group, 20 % (w/w) SCR was added to the basal substrate, based on preliminary trials indicating that 20 % SCR supplementation was the maximum threshold for maintaining normal BSFL growth and development. All substrates were homogenized and vacuum-sealed for storage, and rehydrated with water to 66.7 % moisture content prior to feeding.

Amino acid standard solution (AAS18–5ML) were purchased from Sigma-Aldrich (Steinheim, Germany). All other chemicals were of analytical grade and sourced from Shanghai Macklin Biochemical Technology Co., Ltd. (Shanghai, China) and Shanghai Yuanye Biotechnology Co., Ltd. (Shanghai, China).

2.2. Feeding experiment and sample collection

A total of 2500 four-day-old BSFL were reared in polypropylene containers (30 cm × 20 cm × 10 cm, with 1 mm mesh lids) under controlled conditions (temperature: 27 ± 0.5 °C; relative humidity: 70 %; photoperiod: 12 h light/12 h dark) for 10 days. Each treatment group included three biological replicates. Equal amounts of prepared substrate (500 g dry weight per container) were provided, with feed replenished every 48 h (five feedings in total). The control group data were shared with our previous study (Zhang et al., 2025b).

After the experiment, larvae were separated from residual substrates and transferred to clean containers for a 48-hour starvation period to clear gut contents. Larvae were subsequently rinsed with distilled water to remove surface debris, dried with filter paper, and weighed. Total larval weight and survival rate were recorded, and average individual weights were calculated using random sampling. Processed larvae were immediately stored at −80 °C for subsequent biochemical analyses. Initial and residual substrates from each group were collected, weighed, and dried for mass reduction calculations. All substrate samples were stored at −20 °C until further analysis.

2.3. Growth performance and bioconversion efficiency analysis

The survival rate (%), specific growth rate (% day^{-1}), dry mass reduction of substrate (DMR, %), bioconversion rate (BCR, %), and protein conversion ratio (PCR, %) were calculated according to the formulas provided by Bohm et al. (2022) and Zhang et al. (2025b):

$$\text{Survival rate} = N_f/N_i \times 100 \quad (1)$$

$$\text{Specific growth rate} = \left(\ln W_f - \ln W_i\right)/t \times 100 \quad (2)$$

$$DMR = (DM_{sub} - DM_{res})/DM_{sub} \times 100 \quad (3)$$

$$BCR = DM_{lv}/DM_{sub} \times 100 \quad (4)$$

$$PCR = (DM_{lv} \times Pr_{lv})/(DM_{sub} \times Pr_{sub}) \times 100 \quad (5)$$

Where N_f and N_i represent the final and initial number of larvae. W_f and W_i represent the final and initial weight of larvae (g), t represents the days of rearing. DM_{sub}, DM_{res} and DM_{lv} represent the dry matter of substrate, residue, and larvae biomass (g). Pr_{lv} and Pr_{sub} represent the percentage crude protein of larvae and substrate (%).

2.4. Analysis of proximate and functional components

Comprehensive analyses of proximate and functional components were conducted on BSFL, substrates, and residues across all treatment groups. All proximate component determinations strictly followed AOAC (2005) standard methods, including dry matter (DM), ash, volatile solids, crude protein, and crude fat. Crude protein was measured using a Tecator digestor 2020 (Tecator, Sweden) for digestion, with nitrogen content quantified via a Kjeltec auto sample system 1035 analyzer (Tecator, Sweden), and was calculated using a conversion factor of 6.25 (Lynch and Barbano, 1999). Chitin content was determined according to Black and Schwartz (1950), involving sequential treatments with 2 M HCl and 2 M NaOH (Black and Schwartz, 1950). Total phenolic content was measured using the method described by Pyo et al. (2020), while total sugar content was quantified via acid hydrolysis combined with the 3,5-dinitrosalicylic acid (DNS) method (Miller, 1959). All analyses were performed in triplicate to ensure data reliability.

2.5. Amino acid composition analysis

Amino Acid (AA) composition was determined according to the GB 5009.124–2016 standard method (Ministry of Health of the People's Republic of China, 2016a). The experimental procedure was as follows: Under nitrogen protection, samples were hydrolyzed with 6 mol/L HCl at 110 °C for 22 h. The hydrolysate was freeze-dried, dissolved in 0.02 mol/L sodium citrate buffer, and filtered through a 0.45 μm Millipore membrane. AA composition was analyzed using an Amino Acid Analyzer

l-8900 (HITACHI, Japan).

The essential amino acid index (EAAI) was calculated using Oser's method (Smith, 2017), with reference protein AA composition data sourced from the US Department of Agriculture database. The formula is as follows:

$$EAAI = \sqrt[n]{\frac{aa_1}{AA_1} \times \frac{aa_2}{AA_2} \times \frac{\cdots}{\cdots} \times \frac{aa_n}{AA_n}} \times 100 \quad (6)$$

aa, the amount of specific essential amino acid; AA, the requirement for the same amino acid for the target animal (growing piglets); n, the total number of amino acids involved in the calculation.

2.6. Physicochemical analysis of BSFLO

2.6.1. FA composition analysis

Fatty acid methyl esters (FAMEs) were prepared and quantified following the GB 5009.168–2016 standard method (Ministry of Health of the People's Republic of China, 2016b). Analysis was performed using an Agilent 7890B gas chromatograph (Santa Clara, CA, USA) equipped with a flame ionization detector (FID) and *An sp*-2330 capillary column (100 *m* × 0.25 mm × 0.20 μm). FA identification was achieved by comparing retention times with a 37-component FAME standard mix (Supelco, USA). FA content was calculated via peak area normalization and expressed as a percentage of total FAs.

To evaluate FA accumulation efficiency in larvae, the retention value (Ret_{lv}) was calculated according to Zhang et al. (2025b):

$$Ret_{lv} = FA_{lv}/FA_{sub} \quad (7)$$

FA_{lv}, the total amount of a specific FA in the larval biomass; FA_{sub}, the total amount of the same FA in the initial substrate.

2.6.2. FT-IR analysis

Molecular characterization of BSFLO was conducted using a Nicolet iS50 FT-IR spectrometer (ThermoFisher Scientific, USA). Spectra were recorded ranging from 400 to 4000 cm^{-1} at a resolution of 2 cm^{-1}, with data processed via OMNIC software.

2.6.3. DSC analysis

Phase transition behavior was analyzed using a TGA/DSC1 instrument (Mettler Toledo, Switzerland). Samples (20 mg) were heated from 25 °C to 600 °C at 5 °C/min under nitrogen flow (20 mL/min).

2.6.4. TGA

Thermal stability was assessed using the same TGA/DSC1 instrument under identical conditions (Section 2.6.3).

2.6.5. XRD analysis

Crystal structure analysis was performed using a Bruker-D8 ADVANCE diffractometer (Bruker, Germany) with Cu Kα radiation (40 kV, 150 mA). Scans were conducted from 10° to 45° (2θ) at a rate of 10°/min.

2.7. Antioxidant activity assays

Antioxidant indices of BSFL were measured using specific assay kits from Beijing Solarbio Science & Technology Co.,Ltd. (Beijing, China), following the manufacturer's protocols. These indices included total antioxidant capacity (T-AOC; Kit BC1315), 2,2′-Azino-bis(3-ethylbenzothiazoline-6-sulfonic acid) (ABTS) radical scavenging activity (Kit BC4755), hydroxyl radical (·OH) scavenging capacity (Kit BC1325), superoxide dismutase (SOD) activity (Kit BC5165), and malondialdehyde (MDA) content (Kit BC0025).

2.8. Metabolic profiling

Untargeted metabolomics was performed using a UPLC-MS/MS system. Samples (25 mg) were homogenized with magnetic beads, internal standards, and methanol: acetonitrile: water (2:2:1, v/v), incubated at −20 °C, centrifuged, and freeze-dried. Reconstituted QC samples were analyzed using a Waters UPLC I-Class Plus system coupled to a Q Exactive mass spectrometer. Separation was achieved on a BEH C18 column, with mobile phases of 0.1 % formic acid in water (A) and methanol (B) for positive mode, and 10 mM ammonium formate (A) and 95 % methanol with 10 mM ammonium formate (B) for negative mode. MS parameters included an *m/z* range of 70–1050, resolution of 70,000, and normalized collision energies of 20/40/60 eV. Data were processed using Compound Discoverer 3.3 with mzCloud and ChemSpider databases, and functionally annotated via KEGG.

2.9. Statistical analysis

Data are presented as mean ± standard error (SE) from triplicate measurements. Statistical analyses (one-way ANOVA; $p < 0.05$) were performed using SPSS 26.0 (IBM Corp., USA). Visualization was conducted with GraphPad Prism 9.0.0 (GraphPad Software, USA) and R 4.1.3 (packages: ggplot2).

3. Results and discussion

3.1. Growth performance and bioconversion efficiency

The addition of SCR significantly enhanced the growth performance and bioconversion efficiency of BSFL (Fig. 1). The final larval weight in the SCR group (245.72 g) increased by 7.5 % compared to the control group (228.50 g; $p < 0.001$), with individual larval weight also significantly higher (103.33 mg vs. CG: 96.93 mg; $p < 0.001$). These results align with El-Dakar et al. (2020), who reported that the high lipid and protein content in SCR effectively promotes larval growth. Similarly, Ceccotti et al. (2022) observed a 3-day reduction in BSFL development time when 10 % SCR was added to brewer's spent grain, further supporting the growth-promoting effects of SCR.

Although the survival rate of the SCR group (84.93 %) was only marginally higher than CG (84.19 %; $p = 0.011$), the specific growth rate (50.99 % day^{-1}) increased significantly ($p < 0.001$), likely due to the provision of essential fatty acids (e.g., DHA and EPA) in SCR accelerating larval metabolism (St-Hilaire et al., 2007). The DM content of the SCR group residue (193.88 g) was higher than CG (118.13 g; $p < 0.001$), and the DMR of the SCR group (61.22 %) was significantly lower than CG (76.37 %; $p < 0.001$), consistent with Lin et al. (2022), who noted that antinutritional factors in algal substrates may inhibit complete substrate degradation. Similar trends have been observed in BSFL processing of lignocellulosic waste, where substrate complexity reduces DMR (Abro et al., 2020).

The BCR (15.73 %) and PCR (45.31 %) of the SCR group increased by 19.9 % and 21.6 %, respectively, compared to CG ($p < 0.05$). These findings are comparable to Xiao et al. (2018), who achieved a 12.7 % BCR improvement using *Bacillus subtilis*, but the higher gains here may reflect the ω−3 FA enrichment in SCR. While the PCR of the SCR group (45.31 %) exceeded traditional substrates like wheat bran and soybean meal (27.31–40.99 %) (Zhang et al., 2025a), it remained lower than larvae fed sheep manure (56.3 %) (Lalander et al., 2019). The PCR enhancement may be linked to microbial synergism; for instance, Shukla et al. (2018) demonstrated that mixed microbial consortia elevate protease activity, thereby improving AA utilization. Future studies should integrate microbial pretreatment (e.g., *B. subtilis*) to optimize protein absorption (Gu et al., 2024).

The high BCR and PCR of the SCR group highlight its suitability for scaling ω−3 enriched BSFL production. BSFL processing reduces carbon footprints (Hazarika and Kalita, 2023; van Huis and Gasco, 2023), and

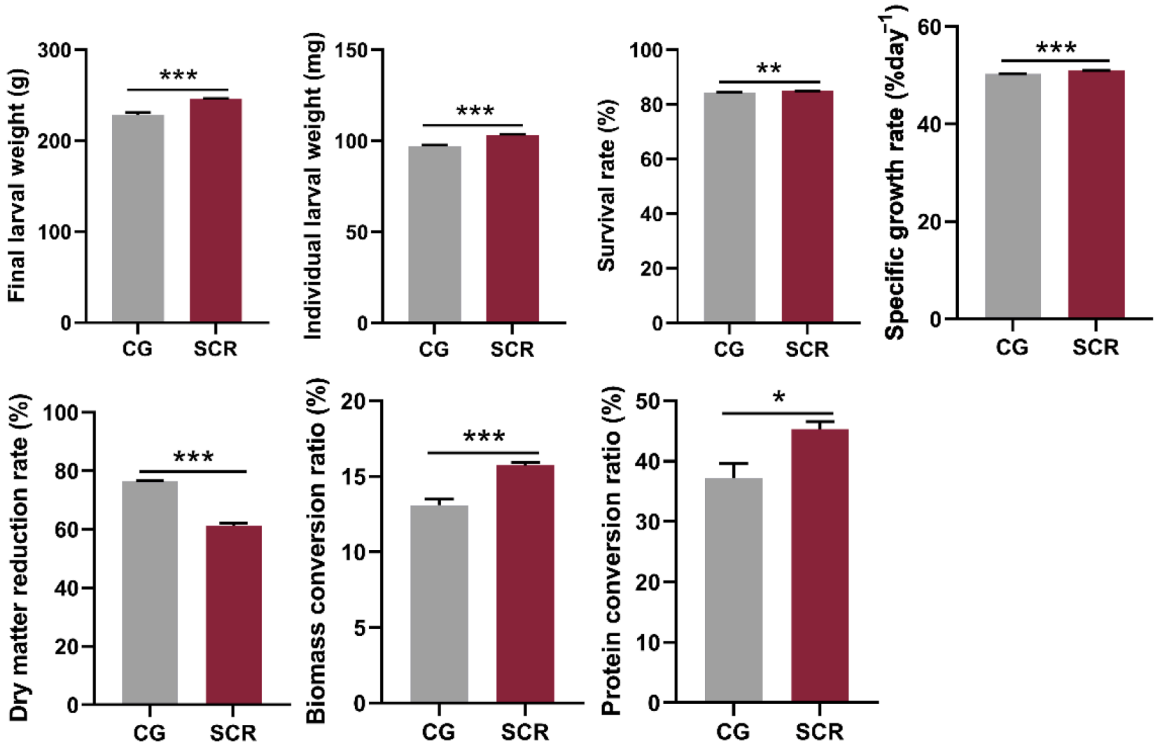

Fig. 1. Growth performance and bioconversion efficiency of black soldier fly larvae (BSFL) reared on different substrates. Data are expressed as mean ± SE ($n = 3$). Significant differences between groups are indicated as $^{*}p < 0.05$, $^{**}p < 0.01$, $^{***}p < 0.001$. CG, control group; SCR, treatment group supplemented with *Schizochytrium* residues.

the improved bioconversion efficiency observed here further supports this advantage. However, the lower DMR may increase substrate processing costs, necessitating optimization through substrate blending (e.g., adding easily degradable agricultural waste) or microbial augmentation (e.g., cellulolytic bacteria; Almutairi et al., 2023).

3.2. Proximate composition and functional components

SCR addition significantly altered the proximate composition and functional components of BSFL (Fig. 2). The DM content of the SCR group (32.01 %) was higher than CG (28.70 %; $p = 0.0087$), possibly due

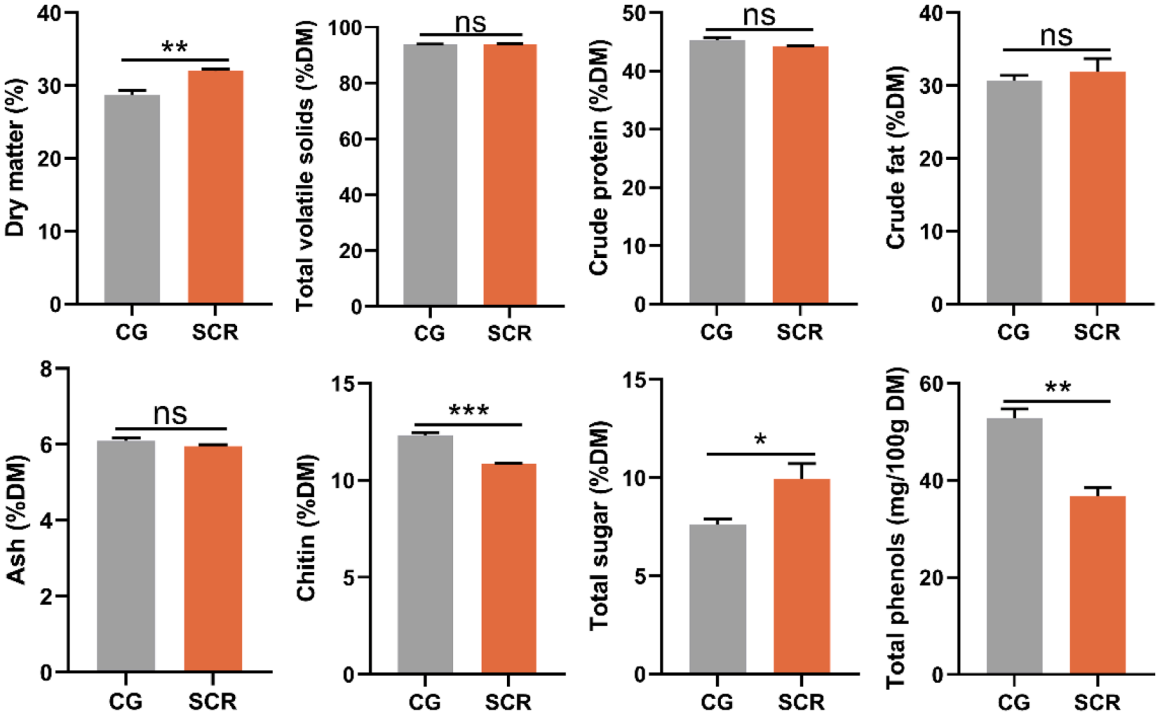

Fig. 2. Proximate composition and functional components of BSFL reared on different substrates. Data are expressed as mean ± SE ($n = 3$). Significant differences between groups are indicated as $^{*}p < 0.05$, $^{**}p < 0.01$, $^{***}p < 0.001$; ns, no significant differences ($p \geq 0.05$).

to the fibrous structure of SCR reducing substrate water-holding capacity (Ceccotti et al., 2022). Similarly, Almutairi et al. (2023) reported increased DM in BSFL fed glycerol waste, suggesting substrate physical properties influence moisture distribution. Volatile solids showed no significant difference between groups (SCR: 94.04 % vs. CG: 93.91 %; $p > 0.05$), indicating SCR did not increase volatile organic losses, consistent with Lalander et al. (2019) using sheep manure.

Crude protein in the SCR group (44.31 % DM) was slightly lower than CG (45.29 % DM; $p = 0.065$), likely due to protease inhibitors in SCR impairing protein absorption. Similar crude protein reductions have been reported in BSFL fed cyanobacterial substrates (Lalander et al., 2019). Conversely, crude fat showed no significant difference (SCR: 31.88 % DM vs. CG: 30.68 % DM; $p > 0.05$), contrasting with El-Dakar et al. (2020), where 50 % SCR elevated lipid content by 15 %, suggesting a substrate ratio threshold for lipid enrichment.

Chitin content in the SCR group (10.84 % DM) decreased by 12 % compared to CG (12.31 % DM; $p < 0.001$), potentially due to carbon metabolic reallocation. Almutairi et al. (2023) noted that high-carbon substrates prioritize lipid synthesis over structural components like chitin. Total phenolic in the SCR group (36.75 mg/100 g DM) was significantly lower than CG (52.81 mg/100 g DM; $p = 0.0018$), which may reduce antioxidant capacity. However, compensatory mechanisms, such as elevated SOD activity under oxidative stress (Abdelfattah and El-Bassiony, 2022) or algal-derived antioxidants (Lin et al., 2022) may mitigate this effect.

The high DM and total sugar of the SCR group suggest its potential as a biofuel feedstock, particularly for ethanol fermentation (Almutairi et al., 2023). However, reduced chitin content may limit chitosan production applications. Stable ash content (SCR: 5.96 % vs. CG: 6.09 %; $p > 0.05$) indicates minimal impact on mineral metabolism, meeting feed stability requirements. Further evaluation of microcystin-LR (MC-LR) residues is warranted (Lin et al., 2022).

3.3. Amino acid profile

SCR addition significantly modified the AA composition of BSFL (Fig. 3). Glycine (Gly) content in the SCR group (46.12 mg/g) increased by 120 % compared to CG (20.96 mg/g; $p = 0.002$), likely due to SCR providing Gly precursors for larval metabolism (Gold et al., 2018). This aligns with microbial-assisted studies where mixed consortia enhanced non-essential amino acid (NEAA) synthesis (Shukla et al., 2018). However, cysteine (Cys) content decreased significantly to 1.02 mg/g (CG: 28.58 mg/g; $p < 0.001$), possibly due to glucosinolates in SCR inhibiting sulfur-containing AA synthesis.

Among essential amino acids (EAAs), valine (Val) and isoleucine (Ile) in the SCR group increased to 36.90 mg/g (CG: 2.55 mg/g; $p < 0.001$) and 24.09 mg/g (CG: 19.40 mg/g; $p = 0.020$), respectively, suggesting microbial synergy promotes branched-chain AA accumulation (Steger et al., 2007). Conversely, methionine (Met) and lysine (Lys) decreased to 11.28 mg/g (CG: 16.34 mg/g; $p = 0.004$) and 39.46 mg/g (CG: 45.42 mg/g; $p = 0.004$), respectively. Notably, the EAAI of the SCR group (50.75) surpassed CG (38.49; $p < 0.001$), indicating improved amino acid balance closer to ideal protein sources.

The optimized AA profile (e.g., elevated EAAI) positions SCR-fed BSFL as a high-quality protein source for poultry and aquaculture feeds. However, Met and Lys deficiencies require mitigation through formulation adjustments, such as blending with soybean meal (Met: 1.18–1.25 %) or synthetic Lys supplements.

3.4. Physicochemical properties of bsflo

3.4.1. Fatty acid profile

The addition of SCR significantly altered the FA profile of BSFL (Fig. 4). The C12:0 content in the SCR group (22.30 %) was significantly lower than in the CG group (33.03 %; $p < 0.001$), while palmitic acid (C16:0) content increased markedly (21.33 % vs. CG: 8.51 %; $p <$

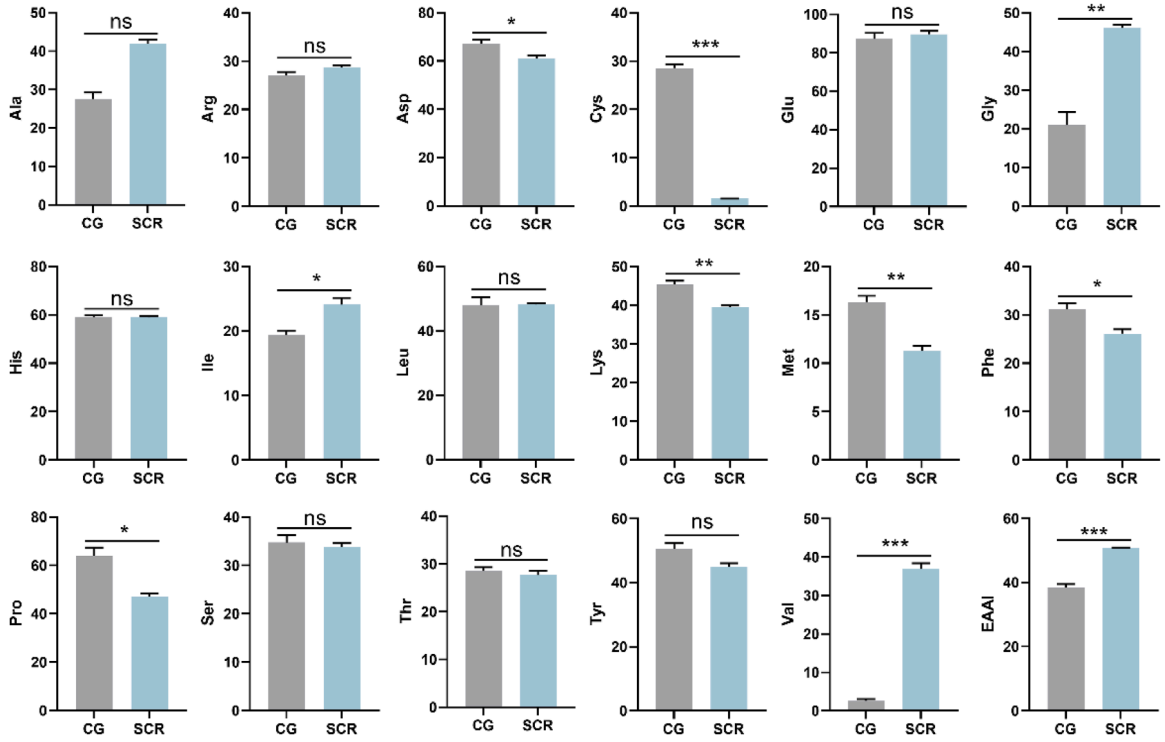

Fig. 3. Amino acid profile (mg/g dry weight) of BSFL reared on different substrates. Data are expressed as mean ± SE ($n = 3$). Significant differences between groups are indicated as $^{*}p < 0.05$, $^{**}p < 0.01$, $^{***}p < 0.001$; ns, no significant differences ($p \geq 0.05$). Abbreviations: Ala, alanine; Arg, arginine; Asp, aspartic acid/asparagine; Cys, cysteine; Glu, glutamic acid/glutamate; Gly, glycine; His, histidine; Ile, isoleucine; Leu, leucine; Lys, lysine; Met, methionine; Phe, phenylalanine; Pro, proline; Ser, serine; Thr, threonine; Tyr, tyrosine; Val, valine; EAAI, essential amino acid index.

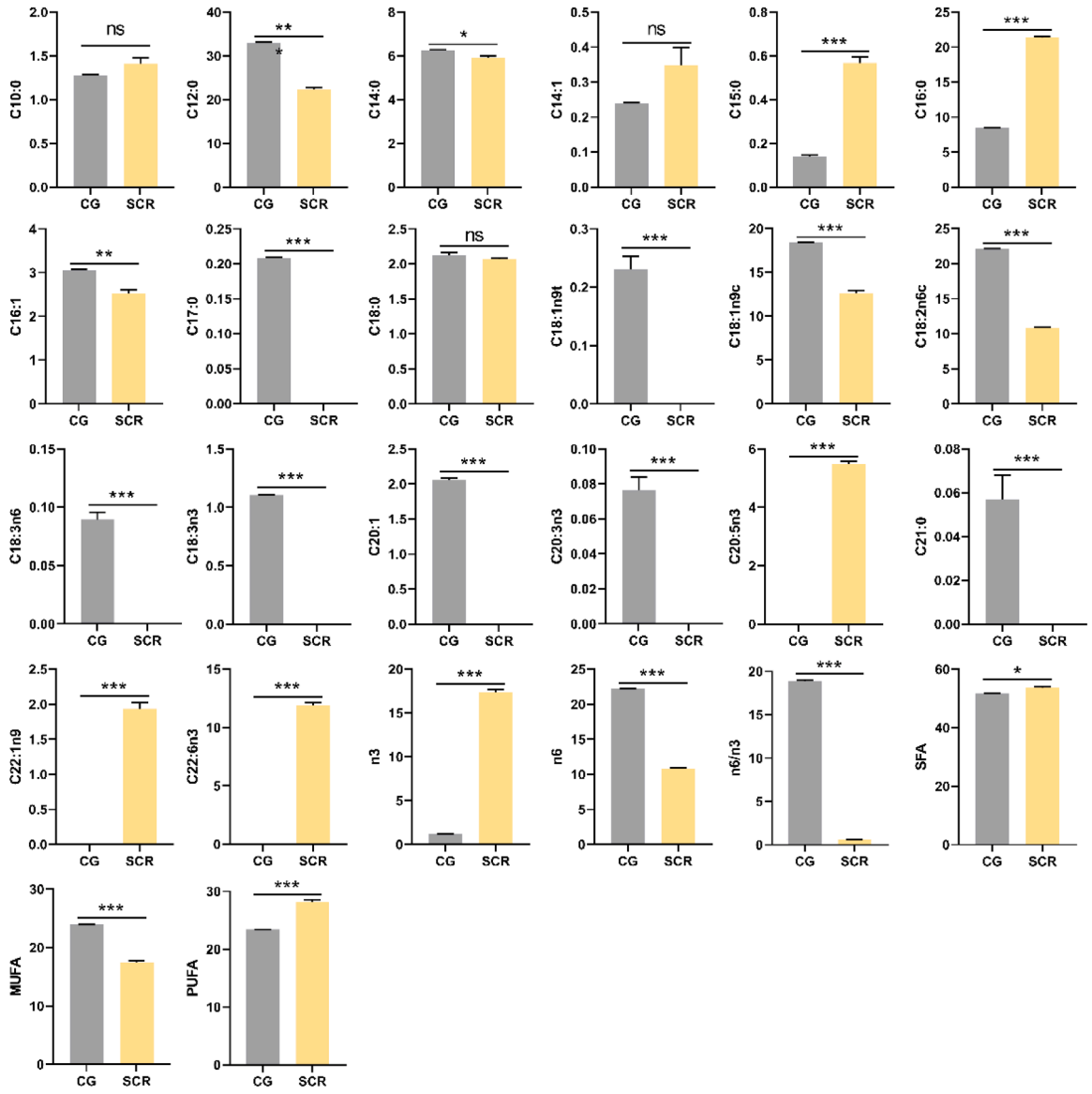

Fig. 4. Fatty acid profile (% total fatty acids) of BSFL reared on different substrates. Data are expressed as mean ± SE ($n = 3$). Significant differences between groups are indicated as $^{*}p < 0.05$, $^{**}p < 0.01$, $^{***}p < 0.001$; ns, no significant differences ($p \geq 0.05$). Abbreviations: SFA, sum of C10:0, C12:0, C14:0, C15:0, C16:0, C17:0, C18:0, C21:0; MUFA, sum of C14:1, C16:1, C18:1n9t, C18:1n9c, C20:1, C22:1n9; PUFA, sum of C18:2n6c, C18:3n6, C18:3n3, C20:3n3, C20:5n3, C22:2n6, C22:6n3; n3, sum of C18:3n3, C20:3n3, C20:5n3, C22:6n3; n6, sum of C18:2n6c, C18:3n6, C22:2n6.

0.001). These results align with El-Dakar et al. (2020), who observed reduced C12:0 levels upon SCR supplementation, likely due to competitive inhibition of medium-chain FA elongase activity by DHA (Guillou et al., 2010). The inherent abundance of C16:0 in SCR (Zhu et al., 2017) may promote its accumulation via direct assimilation or activation of fatty acid synthase (FAS) (Haritos et al., 2014).

A notable enrichment of ω−3 polyunsaturated fatty acids (PUFAs) was observed in the SCR group. EPA and DHA, undetected in CG, reached 5.47 % and 11.90 % in SCR ($p < 0.001$), respectively. This aligns with El-Dakar et al. (2020), who reported SCR-induced ω−3 FA enrichment (5.33–11.80 %), and surpasses Ceccotti et al. (2022), where 10 % SCR yielded only 6.7 % DHA, suggesting higher SCR ratios enhance ω−3 accumulation. Total ω−3 content in SCR increased to 17.37 % (CG: 1.18 %; $p < 0.001$), with the n-6/n-3 ratio decreasing from 18.84 to 0.62 ($p < 0.001$), well below the recommended threshold for health benefits (< 5) (Oonincx et al., 2020; Saini and Keum, 2018), indicating SCR-fed BSFLO is promising as a functional feed additive.

Linoleic acid (C18:2n6c) decreased significantly in SCR (10.83 % vs. CG: 22.13 %; $p < 0.001$), likely due to ω−3 FA-mediated negative feedback on Δ6-desaturase activity, suppressing n-6 metabolism (Saini and Keum, 2018). Monounsaturated fatty acids (MUFAs) also declined (SCR: 17.44 % vs. CG: 23.99 %; $p < 0.001$), possibly linked to substrate-dependent regulation of fatty acid desaturase (FAD) activity. Conversely, total PUFA content rose in SCR (28.20 % vs. CG: 23.40 %; $p < 0.001$), driven by ω−3 enrichment.

The high DHA (11.90 %) and low n-6/n-3 ratio (0.62) in SCR suggest BSFLO is suitable as a premium aquafeed ingredient (Wu et al., 2021), particularly for species like salmon with high ω−3 demands. However, reduced C12:0 may compromise antimicrobial properties (Suryati et al., 2023).

FA retention rates were significantly altered by SCR (Fig. 5). Medium-chain saturated fatty acids (SFAs, e.g., C12:0, C14:0, C15:0) exhibited lower retention in SCR compared to CG. C12:0 retention dropped from 417.08 in CG to 51.62 in SCR ($p < 0.001$; 87.6 % reduction), likely due to FAS inhibition or β-oxidation activation. Similarly, myristic acid (C14:0) and pentadecanoic acid (C15:0) retention

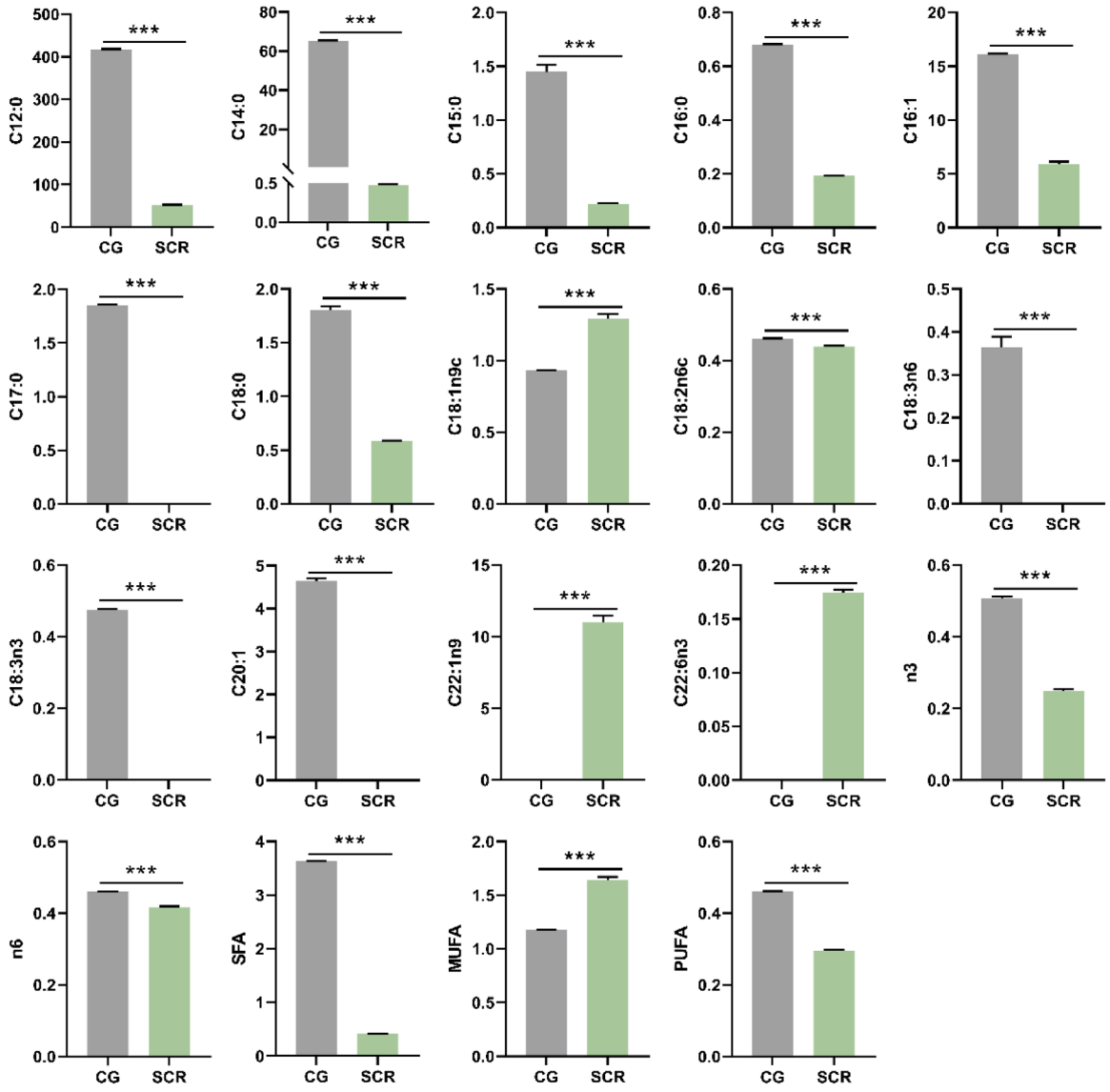

Fig. 5. Retention efficiency (%) of fatty acids of BSFL reared on different substrates. Data are expressed as mean ± SE ($n = 3$). Significant differences between groups are indicated as $^{*}p < 0.05$, $^{**}p < 0.01$, $^{***}p < 0.001$. Abbreviations: SFA, sum of C10:0, C12:0, C14:0, C15:0, C16:0, C17:0, C18:0, C21:0; MUFA, sum of C14:1, 16:1, C18:1n9t, C18:1n9c, C20:1, C22:1n9; PUFA, sum of C18:2n6c, C18:3n6, C18:3n3, C20:3n3, C20:5n3, C22:2n6, C22:6n3; n3, sum of C18:3n3, C20:3n3, C20:5n3, C22:6n3; n6, sum of C18:2n6c, C18:3n6, C22:2n6.

decreased by 99.3 % and 84.8 % ($p < 0.001$), contrasting with Almutairi et al. (2023), where glycerol waste elevated C12:0, highlighting substrate-specific FA metabolism.

While DHA detection confirms SCR's potential as an ω−3 precursor, its low retention (0.17) underscores the need for substrate optimization or microbial synergism. Reduced SFA retention in SCR (0.41 mg/g vs. CG: 3.63 mg/g; $p < 0.001$) may limit biodiesel suitability (Salomone et al., 2017).

3.4.2. FT-IR spectroscopy

FT-IR spectra (Fig. 6A) revealed distinct differences between CG and SCR groups. The peak at 3009 cm^{-1} corresponds to unsaturated C—H stretching vibrations, showed higher absorbance in SCR, indicating reduced unsaturation. BSFL may prioritize SFA retention while partially degrading PUFAs during intestinal oxidation (Roosta et al., 2014). The strong ester bond ($C = O$) peak at 1745 cm^{-1} showed no significant difference, suggesting SCR minimally affects triglyceride core structures. However, SCR exhibited higher absorbance at 1163 cm^{-1} (C—O ester stretching) and 721 cm^{-1} (CH_2 rocking of SFAs), implying SCR promotes short and medium chain FAs synthesis. In summary, FT-IR data indicate SCR alters BSFLO's chemical structure, reducing unsaturation, increasing short and medium chain FAs.

3.4.3. DSC analysis

DSC thermograms (Fig. 6B) revealed distinct heat flow curves between groups. SCR exhibited a larger peak area near 55 °C and higher peak differential (CG: 1.34 W/g vs. SCR: 2.70 W/g), indicating increased high-melting triglycerides or stable crystalline forms, consistent with elevated C16:0. The broad SCR peak (25–300 °C) suggests compositional complexity and enhanced processing adaptability. The thermal decomposition peak temperature increased by 9.6 °C in SCR (CG: 531.1 °C vs. SCR: 540.7 °C). Kissinger equation-derived activation energy (Ea) for SCR (128.6 kJ/mol) was 11.4 % higher than CG (115.4 kJ/mol), confirming SCR improves thermal stability.

3.4.4. TGA analysis

Weight retention curves (Fig. 6C) supported the observed differences in thermal stability. At elevated temperatures, the SCR group

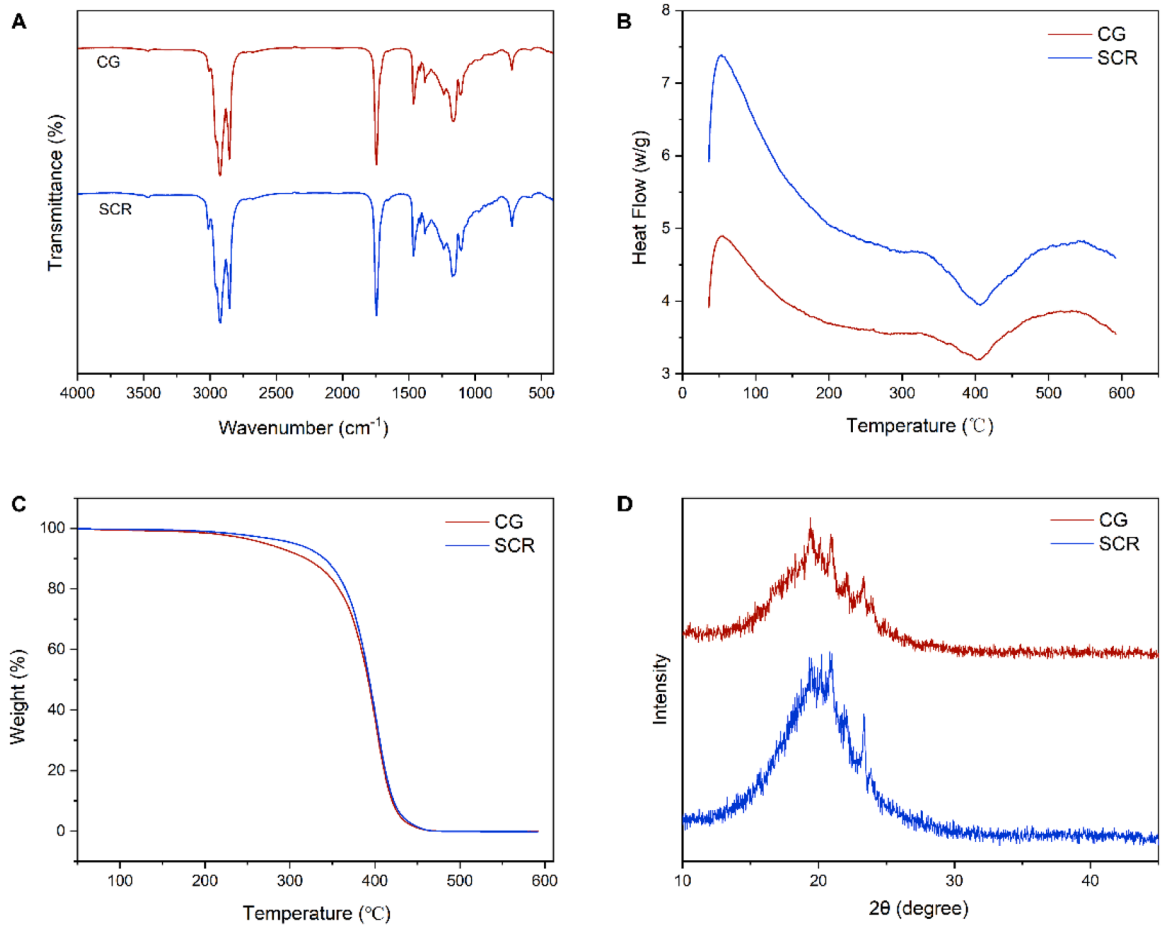

Fig. 6. Physicochemical characterization of BSFL oil. (A) Fourier transform infrared (FT-IR) spectra, (B) differential scanning calorimetry (DSC) thermograms, (C) thermogravimetric analysis (TGA) profiles, and (D) X-ray diffraction (XRD) patterns.

demonstrated superior thermal stability with higher retained mass compared to CG throughout the 50–450 °C range, likely due to delayed decomposition from high-melting SFAs (C16:0) and cross-linking by oxidized PUFAs (Hassan, 2012). For industrial applications, SCR's high retention at > 80 °C supports high-temperature processing (e.g., biodiesel production).

3.4.5. *X-ray diffraction analysis*

XRD patterns (Fig. 6D) showed distinct crystalline features. CG displayed a strong β-polymorph peak at 19.8° (d = 4.46 Å), while SCR exhibited a sharp β'-polymorph peak at 21.5° (d = 4.13 Å), associated with medium-chain FA enrichment (Torbica et al., 2020), consistent with FT-IR data. SCR exhibited a distinct diffraction peak at 23.7° (d = 3.75 Å) with higher intensity than CG, indicating enhanced crystalline ordering in this phase.

The reduced unsaturation (FA profile), enhanced thermal stability (DSC/TGA), and β'-polymorph dominance (XRD) collectively demonstrate SCR modulates BSFLO's physicochemical properties. While medium-chain FAs and β'-crystals improve plasticity, oxidative sensitivity from DHA necessitates antioxidant strategies.

3.5. *Antioxidant capacity*

The addition of SCR significantly altered the antioxidant properties of BSFL slurry (Fig. 7). T-AOC in the SCR group drastically decreased compared to the control group (0.01 mmol/g vs. 0.84 mmol/g; p < 0.001), while ABTS radical scavenging activity significantly increased (63.87 % vs. 47.10 %; p = 0.002). SOD activity also rose markedly (746.36 U/g vs. 505.71 U/g; p = 0.045). However, ·OH scavenging showed no significant difference (SCR: 86.70 % vs. CG: 89.06 %; p > 0.05). Notably, MDA content in the SCR group surged (> 22-fold) compared to CG (168.73 nmol/g vs. 7.65 nmol/g; p < 0.001), indicating severe lipid peroxidation.

The decline in T-AOC may stem from oxidative stress factors in SCR. Lin et al. (2022) demonstrated that MC-LR in cyanobacterial substrates suppresses larval antioxidant systems, reducing total antioxidant capacity. Similarly, Abdelfattah & El-Bassiony (2022) observed that malathion contamination lowers BSFL antioxidant enzyme activity while elevating oxidative damage markers. Despite reduced T-AOC, the elevated SOD activity in SCR suggests a compensatory mechanism. The enhanced ABTS scavenging may reflect direct radical neutralization by carotenoids or polyphenols in SCR. The dramatic MDA increase highlights severe oxidative damage, likely driven by SCR's high PUFA content (prone to lipid peroxidation) and heavy metals (e.g., Cu, Fe) that catalyze hydroxyl radical generation via Fenton reactions (Abdelfattah and El-Bassiony, 2022). Although elevated SOD partially mitigates O_2^- toxicity, it fails to fully suppress lipid peroxidation, necessitating adjunct antioxidants (e.g., vitamin E) to optimize redox balance.

While SCR offers advantages in ABTS scavenging and SOD activity, its high MDA content raises concerns for long-term feed safety. Future studies should integrate microbial augmentation (e.g., *Bacillus subtilis*) to degrade algal-derived oxidative stressors and enhance endogenous antioxidant systems. Additionally, freeze-drying or microencapsulation may stabilize slurry antioxidant properties for extended shelf life.

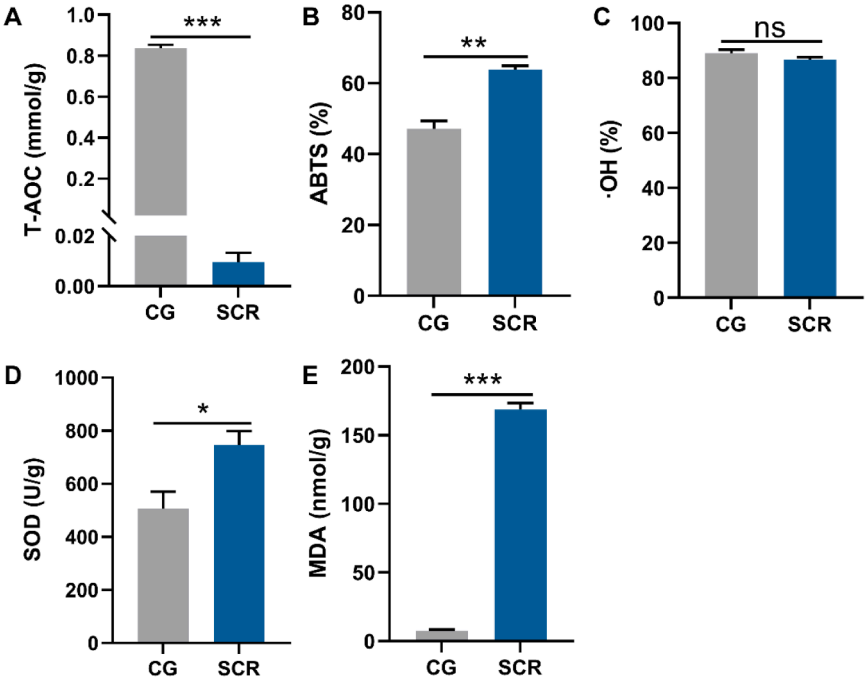

Fig. 7. Antioxidant properties of BSFL slurry. (A) Total antioxidant capacity (T-AOC), (B) 2,2′-Azino-bis(3-ethylbenzothiazoline-6-sulfonic acid) (ABTS) radical scavenging activity, (C) hydroxyl radical (·OH) scavenging activity, (D) superoxide dismutase (SOD) activity, and (E) malondialdehyde (MDA) concentration. Data are expressed as mean ± SE ($n = 3$). Significant differences between groups are indicated as $^{*}p < 0.05$, $^{**}p < 0.01$, $^{***}p < 0.001$; ns, no significant differences ($p \geq 0.05$).

3.6. Metabolomic analysis

Untargeted metabolomics revealed SCR's profound impact on BSFL metabolic profiles. Principal component analysis (PCA) showed clear separation between SCR and CG groups (PC1: 57.04 %, PC2: 37.91 %; Fig. 8A), indicating SCR-driven metabolic reprogramming. Among 1750 annotated metabolites, 743 exhibited significant differential expression ($\log_2$ fold-change ≥ 1.2 or ≤ 0.83, q-value < 0.05), with 390 upregulated and 353 downregulated in SCR (Fig. 8B). The heatmap revealed significant separation between groups (Fig. 8C).

The pantothenate and CoA biosynthesis pathway (map00770) was significantly activated (enrichment factor = 0.18, $p = 6.79\times10^{-6}$), with marked accumulation of tricarboxylic acid (TCA) cycle intermediates like citric acid (FC = 1.98, $q = 0.015$) and oxoglutaric acid (FC = 1.98, $q = 0.015$). This suggests SCR enhances energy metabolism, supplying acetyl-CoA precursors for FA synthesis (Satoh et al., 2020). CoA biosynthesis enrichment likely promotes malonyl-CoA production (Leonardi et al., 2005), a critical substrate for FA elongation.

The unsaturated fatty acid biosynthesis pathway (map01040) was notably enriched (enrichment factor = 0.14, $p = 1.22\times10^{-9}$), with SCR elevating ω−3 PUFA-related metabolites, including EPA (FC = 217.79, $q < 0.001$), DHA (FC = 734.98, $q = 0.002$), and their precursor stearidonic acid (C18:4n3; FC = 554.40, $q < 0.001$). However, Gu et al. (2024) reported that algal antinutrients inhibit elongase (Elovl) activity, limiting C18:4n3-to-EPA/DHA conversion.

The alanine, aspartate, and glutamate metabolism pathway (map00250) were also enriched (enrichment factor = 0.32, $p = 3.76\times10^{-12}$; Fig. 8D). l-Glutamic acid (FC = 2.04, $q = 0.015$) increased in SCR, while d-aspartic acid (FC = 0.19, $q = 0.005$) decreased. Reduced d-aspartate may competitively inhibit l-aspartate metabolism in the aspartate-malate shuttle, impairing mitochondrial NADH transfer to the cytosol (Forbes and Cooper, 2012). This could lower cytosolic NADH/-NAD^+ ratios, disrupting malate regeneration in the citrate-pyruvate cycle. Since long-chain FA elongation relies heavily on NADPH (primarily from the pentose phosphate pathway), while short-chain FA synthesis is less NADPH-dependent, this shift may selectively hinder long-chain FA elongation.

Upregulation of the amino acid biosynthesis pathway (map01230) aligns with the 7.5 % increase in larval final weight, consistent with Ceccotti et al. (2022), who observed a 3-day reduction in BSFL development time with 10 % SCR supplementation. However, limitations in NADPH supply inhibited NADPH-dependent amino acid elongation reactions, ultimately suppressing the synthesis of Met, Cys, and Lys.

Collectively, KEGG analysis and metabolite trends suggest that elevated ω−3 PUFA levels in BSFL arise more from direct assimilation of exogenous ω−3 PUFAs than de novo synthesis, supported by: (1) NADPH supply limitations constraining FA elongation. (2) Algal substrate-mediated Elovl inhibition (Gu et al., 2024). To enhance ω−3 PUFA bioconversion, future strategies may involve microbial fermentation, Elovl engineering, or substrate optimization with Δ6-desaturase-rich microbes (e.g., marine algal symbionts). The activation of amino acid biosynthesis pathways underscores BSFL's potential as a high-protein feed. This study provides the first multi-scale mechanistic insights into SCR-driven bioconversion, advancing the development of ω−3-enriched insect products.

Furthermore, future work should involve industrial-scale validation to assess the economic viability and environmental benefits of SCR-fed BSFL as functional feed and food ingredients. Additional studies on the safety of the resulting products are required to advance BSFL bioconversion as a key technology for sustainable resource recovery and high-value product development.

4. Conclusion

This study demonstrates that SCR supplementation in BSFL bioconversion significantly enhances ω−3 FA enrichment (EPA: 5.47 %; DHA: 11.90 %) and reduces the n-6/n-3 ratio to 0.62, meeting health-beneficial thresholds. The resulting BSFLO exhibited higher thermal stability and β'-crystal formation. However, SCR induced oxidative stress despite compensatory SOD activity. Supplementation with SCR significantly enhanced larval growth, while metabolic reprogramming via TCA cycle activation and CoA biosynthesis promoted FA synthesis.

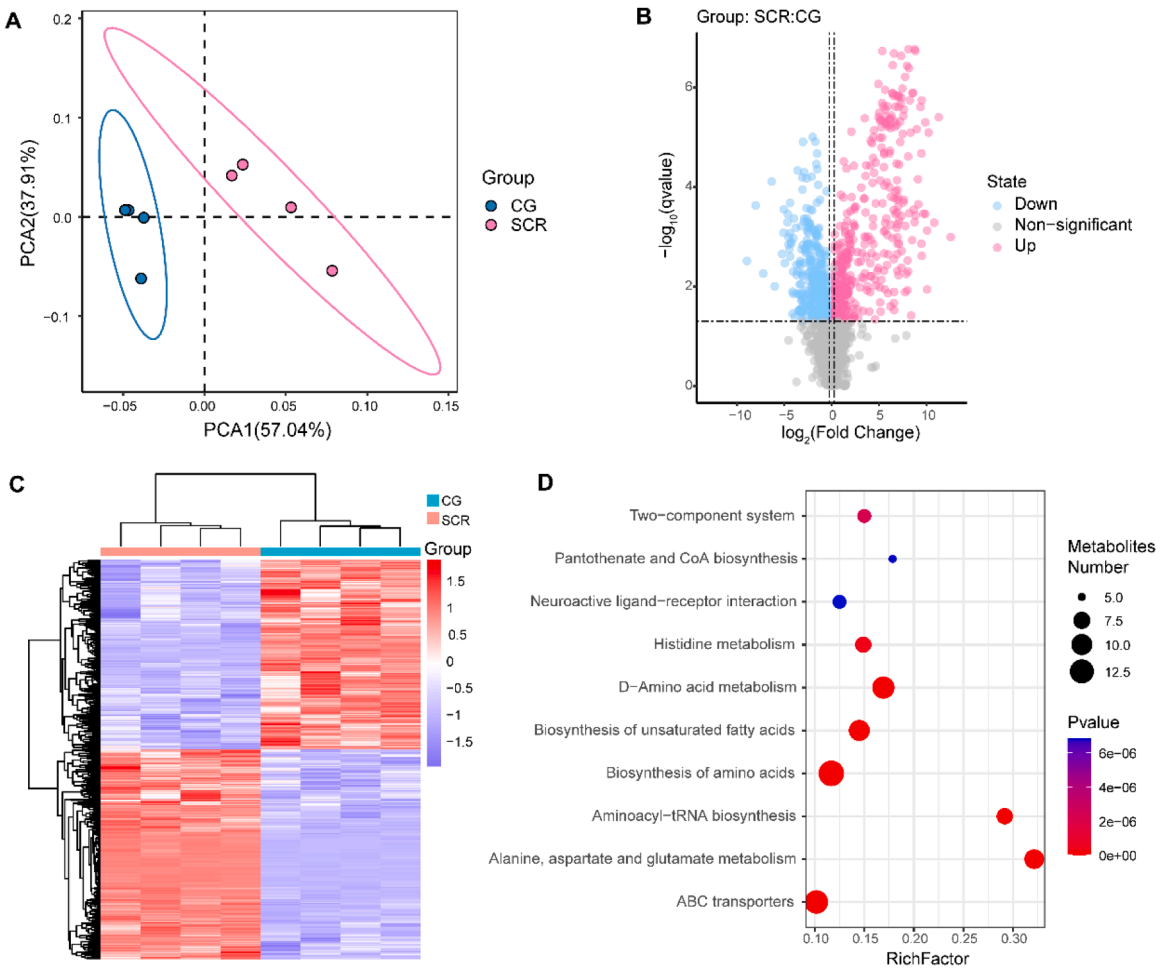

Fig. 8. Metabolic profiling of BSFL reared on different substrates. (A) PCA score plot showing separation between groups (95 % confidence ellipses). (B) Volcano plot of differential metabolites (the x-axis represents the $\log_2$-transformed fold change, and the y-axis represents the -$\log_{10}$-transformed q-value). Red: upregulated; blue: downregulated; gray: nonsignificant. (C) Heatmap of significantly altered metabolites (Z-score normalized intensities). (D) Pathway enrichment analysis bubble plot. Dot size reflects metabolite count; x-axis shows enrichment factor (rich factor).

Metabolomics revealed ω−3 accumulation primarily through exogenous assimilation rather than endogenous synthesis. BSFL-based bioconversion of SCR reduces energy demand and enhances product value, aligning with circular economy goals.

Ethical statement

There are no ethical issues associated with the experimental procedures on insects described in this research article.

Data availability

Data will be made available on request.

CRediT authorship contribution statement

Yaru Zhang: Writing – original draft, Methodology, Formal analysis, Data curation, Conceptualization. **Jing Liu:** Writing – review & editing, Funding acquisition. **Yan Xiao:** Writing – review & editing, Visualization. **He Yang:** Methodology. **Yanzhou Zhang:** Methodology. **Chrysantus Mbi Tanga:** Methodology. **Dawei Huang:** Writing – review & editing, Supervision, Funding acquisition. **Jinhua Xiao:** Writing – review & editing, Supervision, Funding acquisition.

Declaration of competing interest

The authors declare that they have no known competing financial interests or personal relationships that could have appeared to influence the work reported in this paper.

Acknowledgments

This research was supported by the National Natural Science Foundation of China (31830084, 32070466 & 31970440), the National Natural Science Foundation of China (32301412, 32070466, 32200375).

References

Abdelfattah, E.A., El-Bassiony, G.M., 2022. Impact of malathion toxicity on the oxidative stress parameters of the black soldier fly *Hermetia illucens* (Linnaeus, 1758) (Diptera: stratiomyidae). Sci. Rep. 12 (1), 4583. https://doi.org/10.1038/s41598-022-08564-8.

Abro, Z., Kassie, M., Tanga, C., Beesigamukama, D., Diiro, G., 2020. Socio-economic and environmental implications of replacing conventional poultry feed with insect-based feed in Kenya. J. Clean. Prod. 265, 121871. https://doi.org/10.1016/j.jclepro.2020.121871.

Ali, E.M., 2022. Chapter 23 - life cycle assessment for microalgae-derived biofuels. In: El-Sheekh, M., Abomohra, A.E.-F. (Eds.), Handbook of Algal Biofuels. Elsevier, pp. 523–545. https://doi.org/10.1016/B978-0-12-823764-9.00012-1.

Almutairi, A.W., Abomohra, A., Elsayed, M., 2023. A closed-loop approach for enhanced biodiesel recovery from rapeseed biodiesel-based byproducts through integrated

glycerol recycling by black soldier fly larvae. J. Clean. Prod. 409, 137236. https://doi.org/10.1016/j.jclepro.2023.137236.
AOAC, 2005. Official Methods of Analysis of AOAC International, 18th ed. Association of Official Analytical Chemists (AOAC), Gaitherburg, MD.
Barroso, F.G., Sánchez-Muros, M.-J., Segura, M., Morote, E., Torres, A., Ramos, R., Guil, J.-L., 2017. Insects as food: enrichment of larvae of *Hermetia illucens* with omega 3 fatty acids by means of dietary modifications. J. Food Compos. Anal. 62, 8–13. https://doi.org/10.1016/j.jfca.2017.04.008.
Black, M.M., Schwartz, H.M., 1950. The estimation of Chitin and Chitin nitrogen in crawfish waste and derived products. Analyst 75 (889), 185–189. https://doi.org/10.1039/an9507500185.
Bohm, K., Hatley, G.A., Robinson, B.H., Gutiérrez-Ginés, M.J., 2022. Black Soldier Fly-based bioconversion of biosolids creates high-value products with low heavy metal concentrations. Resour. Conserv. Recycl. 180, 106149. https://doi.org/10.1016/j.resconrec.2021.106149.
Ceccotti, C., Bruno, D., Tettamanti, G., Branduardi, P., Bertacchi, S., Labra, M., Rimoldi, S., Terova, G., 2022. New value from food and industrial wastes – Bioaccumulation of omega-3 fatty acids from an oleaginous microbial biomass paired with a brewery by-product using black soldier fly (*Hermetia illucens*) larvae. Waste Manag. 143, 95–104. https://doi.org/10.1016/j.wasman.2022.02.029.
El-Dakar, M.A., Ramzy, R.R., Ji, H., Plath, M., 2020. Bioaccumulation of residual omega-3 fatty acids from industrial *Schizochytrium* microalgal waste using black soldier fly (*Hermetia illucens*) larvae. J. Clean. Prod. 268, 122288. https://doi.org/10.1016/j.jclepro.2020.122288.
El-Dakar, M.A., Ramzy, R.R., Wang, D., Ji, H., 2021. Sustainable management of Se-rich silkworm residuals by black soldier flies larvae to produce a high nutritional value and accumulate ω-3 PUFA. Waste Manag. 124, 72–81. https://doi.org/10.1016/j.wasman.2021.01.040.
Ewald, N., Vidakovic, A., Langeland, M., Kiessling, A., Sampels, S., Lalander, C., 2020. Fatty acid composition of black soldier fly larvae (*Hermetia illucens*) – Possibilities and limitations for modification through diet. Waste Manag. 102, 40–47. https://doi.org/10.1016/j.wasman.2019.10.014.
Forbes, J.M., Cooper, M.E., 2012. Glycation in diabetic nephropathy. Amino Acids. 42 (4), 1185–1192. https://doi.org/10.1007/s00726-010-0771-4.
Gold, M., Tomberlin, J.K., Diener, S., Zurbrügg, C., Mathys, A., 2018. Decomposition of biowaste macronutrients, microbes, and chemicals in black soldier fly larval treatment: a review. Waste Manag. 82, 302–318. https://doi.org/10.1016/j.wasman.2018.10.022.
Gu, P., Chen, L., Yang, K., Ren, X., Zhang, Z., Miao, H., 2024. Improving the conversion efficiency of cyanobacterial biomass and the value of black soldier fly products by inoculating microorganisms. J. Clean. Prod. 464, 142754. https://doi.org/10.1016/j.jclepro.2024.142754.
Guillou, H., Zadravec, D., Martin, P.G.P., Jacobsson, A., 2010. The key roles of elongases and desaturases in mammalian fatty acid metabolism: insights from transgenic mice. Prog, Lipid Res. 49 (2), 186–199. https://doi.org/10.1016/j.plipres.2009.12.002.
Haritos, V.S., Horne, I., Damcevski, K., Glover, K., Gibb, N., 2014. Unexpected functional diversity in the fatty acid desaturases of the flour beetle *tribolium castaneum* and identification of key residues determining activity. Insect Biochem. Mol. Biol. 51, 62–70. https://doi.org/10.1016/j.ibmb.2014.05.006.
Hassan, H.A., 2012. Lipid peroxidation end-products as a key of oxidative stress: effect of antioxidant on their production and transfer of free radicals. In: Catala, A. (Ed.), *Lipid Peroxidation*. IntechOpen. https://doi.org/10.5772/45944.
Hazarika, A.K., Kalita, U., 2023. Human consumption of insects farming edible insects can help improve food security and boost developing economies. Science 379 (6628), 140–141. https://doi.org/10.1126/science.abp8819.
Heffernan, O., 2017. Sustainability: a meaty issue. Nature 544 (7651), S18–S20. https://doi.org/10.1038/544S18a.
Huang, G., Zhang, Y., Liu, F., Xiao, J., Huang, D., 2025. Fatty acid profile of insect oil and regulation mechanism as nutritious and functional oil: an integrative review. J. Food Compos. Anal. 137, 106809. https://doi.org/10.1016/j.jfca.2024.106809.
Lalander, C., Diener, S., Zurbrügg, C., Vinnerås, B., 2019. Effects of feedstock on larval development and process efficiency in waste treatment with black soldier fly (*Hermetia illucens*). J. Clean. Prod. 208, 211–219. https://doi.org/10.1016/j.jclepro.2018.10.017.
Leonardi, R., Zhang, Y.-M., Rock, C.O., Jackowski, S., 2005. Coenzyme A: back in action. Prog, Lipid Res. 44 (2), 125–153. https://doi.org/10.1016/j.plipres.2005.04.001.
Liland, N.S., Biancarosa, I., Araujo, P., Biemans, D., Bruckner, C.G., Waagbo, R., Torstensen, B.E., Lock, E.-J., 2017. Modulation of nutrient composition of black soldier fly (*Hermetia illucens*) larvae by feeding seaweed-enriched media. PLoS. One 12 (8). https://doi.org/10.1371/journal.pone.0183188. Article e0183188.
Lin, T.-H., Wang, D.-H., Zou, H., Zheng, Y., Fu, S.-F., 2022. Effects of salvaged cyanobacteria content on larval development and feedstock humification during black soldier fly larvae (*Hermetia illucens*) composting. Env., Res. 215. https://doi.org/10.1016/j.envres.2022.114401. Article 114401.
Lynch, J.M., Barbano, D.M., 1999. Kjeldahl nitrogen analysis as a reference method for protein determination in dairy products. J. AOAC Int. 82 (6), 1389–1398. https://doi.org/10.1093/jaoac/82.6.1389.
Matsakas, L., Gao, Q., Jansson, S., Rova, U., Christakopoulos, P., 2017. Green conversion of municipal solid wastes into fuels and chemicals. Electron. J. Biotechnol. 26, 69–83. https://doi.org/10.1016/j.ejbt.2017.01.004.
Meneguz, M., Schiavone, A., Gai, F., Dama, A., Lussiana, C., Renna, M., Gasco, L., 2018. Effect of rearing substrate on growth performance, waste reduction efficiency and chemical composition of black soldier fly (*Hermetia illucens*) larvae. J. Sci, Food Agric. 98 (15), 5776–5784. https://doi.org/10.1002/jsfa.9127.
Miller, G.L., 1959. Use of dinitrosalicylic acid reagent for determination of reducing sugar. Anal, Chem 31 (3), 426–428. https://doi.org/10.1021/ac60147a030.
Ministry of Health of the People's Republic of China cmoH, 2016a. National Food Safety Standard-Determination of Amino Acid in Foods. GB 5009.124-2016. a. Standards Press of China, Beijing, China.
Ministry of Health of the People's Republic of China cmoH, 2016b. National Food Safety Standard-Determination of Fatty Acid in Foods. GB 5009.168-2016. b. Standards Press of China, Beijing, China.
Hussain, M.U., Noor, T., Ahmad, A., Nasir, M.S., Khan, M., 2023. Characterization of sweet sorghum accessions for grain-related traits using metabolomics analysis. Agrobiol. Rec. 14, 91–102. https://doi.org/10.47278/journal.abr/2023.041.
Narayanan, M., 2024. Biorefinery products from algal biomass by advanced biotechnological and hydrothermal liquefaction approaches. Discov. Appl. Sci. 6 (4), 146. https://doi.org/10.1007/s42452-024-05777-6.
Noman, M.U., Azhar, S., 2023. Metabolomics, a potential way to improve abiotic stresses tolerance in cereal crops. Int. J. Agric. Biosci. 12 (1), 47–55. https://doi.org/10.47278/journal.ijab/2023.043.
Oonincx, D.G.A.B., Laurent, S., Veenenbos, M.E., van Loon, J.J.A., 2020. Dietary enrichment of edible insects with omega 3 fatty acids. Insect Sci. 27 (3), 500–509. https://doi.org/10.1111/1744-7917.12669.
Panse, M.L., Phalke, S.D., 2016. World Market of omega-3 fatty acids. In: Hegde, M.V., Zanwar, A.A., Adekar, S.P. (Eds.), Omega-3 Fatty Acids: Keys to Nutritional Health. Springer International Publishing, pp. 79–88. https://doi.org/10.1007/978-3-319-40458-5_7.
Pyo, S.J., Kang, D.G., Jung, C., Sohn, H.Y., 2020. Anti-thrombotic, Anti-oxidant and *haemolysis* activities of six edible insect species. Foods. 9 (4). https://doi.org/10.3390/foods9040401. Article 401.
Roosta, M., Ghaedi, M., Daneshfar, A., 2014. Optimisation of ultrasound-assisted reverse micelles dispersive liquid–liquid micro-extraction by Box–Behnken design for determination of acetoin in butter followed by high performance liquid chromatography. Food Chem. 161, 120–126. https://doi.org/10.1016/j.foodchem.2014.03.043.
Saini, R.K., Keum, Y.-S., 2018. Omega-3 and omega-6 polyunsaturated fatty acids: dietary sources, metabolism, and significance — A review. Life Sci. 203, 255–267. https://doi.org/10.1016/j.lfs.2018.04.049.
Salomone, R., Saija, G., Mondello, G., Giannetto, A., Fasulo, S., Savastano, D., 2017. Environmental impact of food waste bioconversion by insects: application of Life Cycle Assessment to process using *Hermetia illucens*. J. Clean. Prod. 140, 890–905. https://doi.org/10.1016/j.jclepro.2016.06.154.
Satoh, S., Ozaki, M., Matsumoto, S., Nabatame, T., Kaku, M., Shudo, T., Asayama, M., Chohnan, S., 2020. Enhancement of fatty acid biosynthesis by exogenous acetyl-CoA carboxylase and pantothenate kinase in *Escherichia coli*. Biotechnol, Lett. 42 (12), 2595–2605. https://doi.org/10.1007/s10529-020-02996-w.
Shah, A.M., Wang, Z.S., Hu, R., Peng, Q.H., Zou, H.W., Wang, L.Z., Xue, B., 2024. Discovery of the enrichment pathways and biomarkers using metabolomics techniques in unilateral and bilateral castration in yellow cattle. Pak Vet J 44 (2), 252–259. https://doi.org/10.29261/pakvetj/2024.166.
Shukla, S.P., Plata, C., Reichelt, M., Steiger, S., Heckel, D.G., Kaltenpoth, M., Vilcinskas, A., Vogel, H., 2018. Microbiome-assisted carrion preservation aids larval development in a burying beetle. Proc. Natl. Acad. Sci. 115 (44), 11274–11279. https://doi.org/10.1073/pnas.1812808115.
Smith, D.M., 2017. Protein separation and characterization procedures. In: Nielsen, S.S. (Ed.), Food Analysis. Springer International Publishing, pp. 431–453. https://doi.org/10.1007/978-3-319-45776-5_24.
Spranghers, T., Ottoboni, M., Klootwijk, C., Ovyn, A., Deboosere, S., De Meulenaer, B., Michiels, J., Eeckhout, M., De Clercq, P., De Smet, S., 2017. Nutritional composition of black soldier fly (*Hermetia illucens*) prepupae reared on different organic waste substrates. J. Sci, Food Agric. 97 (8), 2594–2600. https://doi.org/10.1002/jsfa.8081.
St-Hilaire, S., Cranfill, K., McGuire, M.A., Mosley, E.E., Tomberlin, J.K., Newton, L., Sealey, W., Sheppard, C., Irving, S., 2007. Fish offal recycling by the black soldier fly produces a foodstuff high in omega-3 fatty acids. J. World Aquac. Soc. 38 (2), 309–313. https://doi.org/10.1111/j.1749-7345.2007.00101.x.
Steger, K., Jarvis, Å., Vasara, T., Romantschuk, M., Sundh, I., 2007. Effects of differing temperature management on development of actinobacteria populations during composting. Res, Microbiol. 158 (7), 617–624. https://doi.org/10.1016/j.resmic.2007.05.006.
Suryati, T., Julaeha, E., Farabi, K., Ambarsari, H., Hidayat, A.T., 2023. Lauric acid from the black soldier fly (*Hermetia illucens*) and its potential applications. Sustainability 15 (13), 10383. https://www.mdpi.com/2071-1050/15/13/10383.
Tepper, K., Edwards, O., Sunna, A., Paulsen, I.T., Maselko, M., 2024. Diverting organic waste from landfills via insect biomanufacturing using engineered black soldier flies (*Hermetia illucens*). Commun. Biol. 7 (1), 862. https://doi.org/10.1038/s42003-024-06516-8.
Tzachor, A., Richards, C.E., Holt, L., 2021. Future foods for risk-resilient diets. Nat. Food 2 (5), 326–329. https://doi.org/10.1038/s43016-021-00269-x.
van Huis, A., Gasco, L., 2023. Insects as feed for livestock production insect farming for livestock feed has the potential to replace conventional feed. Science 379 (6628), 138–139. https://doi.org/10.1126/science.adc9165.
Wu, N., Ma, Y., Yu, X., Wang, X., Wang, Q., Liu, X., Xu, X., 2024. Black soldier fly larvae bioconversion and subsequent composting promote larval frass quality during pig and chicken manure transformation process. Bioresour, Technol. 402, 130777. https://doi.org/10.1016/j.biortech.2024.130777.
Wu, Y., Zhang, H., Zhang, R., Cao, G., Li, Q., Zhang, B., Wang, Y., Yang, C., 2021. Serum metabolome and gut microbiome alterations in broiler chickens supplemented with lauric acid. Poult. Sci. 100 (9), 101315. https://doi.org/10.1016/j.psj.2021.101315.
Xiao, X., Mazza, L., Yu, Y., Cai, M., Zheng, L., Tomberlin, J.K., Yu, J., van Huis, A., Yu, Z., Fasulo, S., Zhang, J., 2018. Efficient co-conversion process of chicken manure into

protein feed and organic fertilizer by *Hermetia illucens* L. (Diptera: stratiomyidae) larvae and functional bacteria. J. Env., Manage 217, 668–676. https://doi.org/10.1016/j.jenvman.2018.03.122.

Zhang, Y., Huang, G., Chen, S., Yu, T., Ren, X., Xiao, J., Huang, D., 2025a. Enhanced waste-to-biomass conversion and reduced nitrogen emissions for black soldier fly larvae (*Hermetia illucens*) through modifying protein to energy ratio. J. Env., Manage 373, 123718. https://doi.org/10.1016/j.jenvman.2024.123718.

Zhang, Y., Huang, G., Wei, X., Zhang, Y., Chen, S., Sui, Z., Huang, D., Xiao, J., 2025b. Bioconversion of black soldier fly larvae on agricultural by-products: study on growth, nutrition, physicochemical properties, metabolic profiling, and larvae-substrate component correlations. J. Clean. Prod. 521, 146250. https://doi.org/10.1016/j.jclepro.2025.146250.

Zhu, A., Nowack, L., Jeong, M.Y., 2017. On the production of high-purity docosahexaenoic acid from heterotrophic microalgae. Dep. Chem. Biomol. Eng. 1–387. https://repository.upenn.edu/cbe_sdr/91.